JOURNAL OF Applied Polymer SCIENCE

Functional silk fabric for detection and absorption of Zn(II)

Fuyou Ke, Hao Chen, Shanyi Guang, Hongyao Xu
College of Material Science and Engineering & State Key Laboratory for Modification of Chemical Fibers and Polymer Materials, Donghua University, Shanghai 201620, China
Correspondence to: H. Xu (E-mail: hongyaoxu@163.com)

ABSTRACT: Two reactive dyes (P1 and P2) based on salicyladehyde-4-amino-benzoylhydrazone, which show high sensitivity and selectivity in sensing Zn^{2+}, were synthesized and used to modify nonwoven silk fabrics. The prepared silk fabric was then characterized by IR, UV-Vis, and fluorescence measurements. The results showed that reactive dyes were chemically reacted with silk fibers, rather than physical absorption. Moreover, compared with raw silk fabric, functional silk fabric was bestowed the properties of Zn^{2+} detection and improved absorption capacity of Zn^{2+}. © 2016 Wiley Periodicals, Inc. J. Appl. Polym. Sci. **2016**, *133*, 43952.

KEYWORDS: adsorption; biomaterials; dyes/pigments; fibers; sensors and actuators

Received 21 January 2016; accepted 17 May 2016
DOI: 10.1002/app.43952

INTRODUCTION

Zinc ion is the second most abundant transition metal in the human body. It plays a very important role in many physiological processes.[1] It is well known that disorder of zinc metabolism is closely related to many severe neurological diseases such as Alzheimer's disease and Parkinson's disease.[2,3] Moreover, zinc ions are also important in the environment pollution. Therefore, detection and monitoring of Zn^{2+} in both the environmental and biological systems are highly demanded. Among various analytical methods for ion detection, fluorescent method was the most studied because of its simplicity, cost effectiveness and high sensitivity. In the past decades, many fluorescent probes of Zn^{2+} ion have been developed with various detection mechanisms based on quinoline,[4–7] courmarin,[8–11] naphthalimide,[12] indole,[13] BODIPY,[14–16] bipyridine,[17,18] and other fluorophores.[19–24] However, the previous fluorescent probes are mainly small molecules. In this article, we introduced the fluorescent molecules to silk fibers, which can be further used as fluorescent probes like pH test paper.

Functional fibers refer to the fibers with some special features or for certain applications compared with the conventional fibers. They are mainly divided into three categories: The first category is modified conventional synthetic fibers to overcome its inherent shortcomings, also known as differential fibers; the second is modified fibers with new features, such as conductivity, water absorption, moisture, antibacterial, deodorant, fragrance, flame retardant, UV shielding, and other additional properties; the third category is high-performance fibers, which show excellent performance including high strength, high modulus, high temperature resistance, and chemical resistance. Here we focus on functional fibers of the second category. The common methods of fiber modification include plasma technology, heat, light radiation, coatings, absorption, and self-assembly. Silk fibroin (SF) derived from silkworm cocoon has many excellent properties, including good biocompatibility and biodegradability, excellent mechanical properties, as well as abundant source. Because of its easy processing, SF can be made into various forms, including films,[25] hydrogels,[26] nonwoven fabrics,[27] and 3D porous scaffolds.[28] Moreover, compared with cellulose, SF has amino groups besides hydroxyl groups, which makes SF very feasible to be modified. Tang *et al.* introduced silver nanoparticles into SF fibers by adsorption to prepare functional SF fibers with excellent antibacterial properties.[29] Recently, our group prepared SF scaffolds with two-photon fluorescence emission and white-light emitting properties based on molecular recognition and materials assembly technique.[30–32] The fabricated scaffold materials exhibited improved optical properties, which was very promising in biomedical applications. However, the previous modification methods were mainly nonvalent, while covalent modification of SF fibers will enhance the stability of their functionality.

Here, two reactive dyes based on salicyladehyde-4-amino-benzoylhydrazone were designed and synthesized. Then SF fabrics were functionalized by these dyes via chemical bonding. The functional SF fabrics were well characterized and their applications in absorption and detection of Zn^{2+} were investigated.

Additional Supporting Information may be found in the online version of this article.

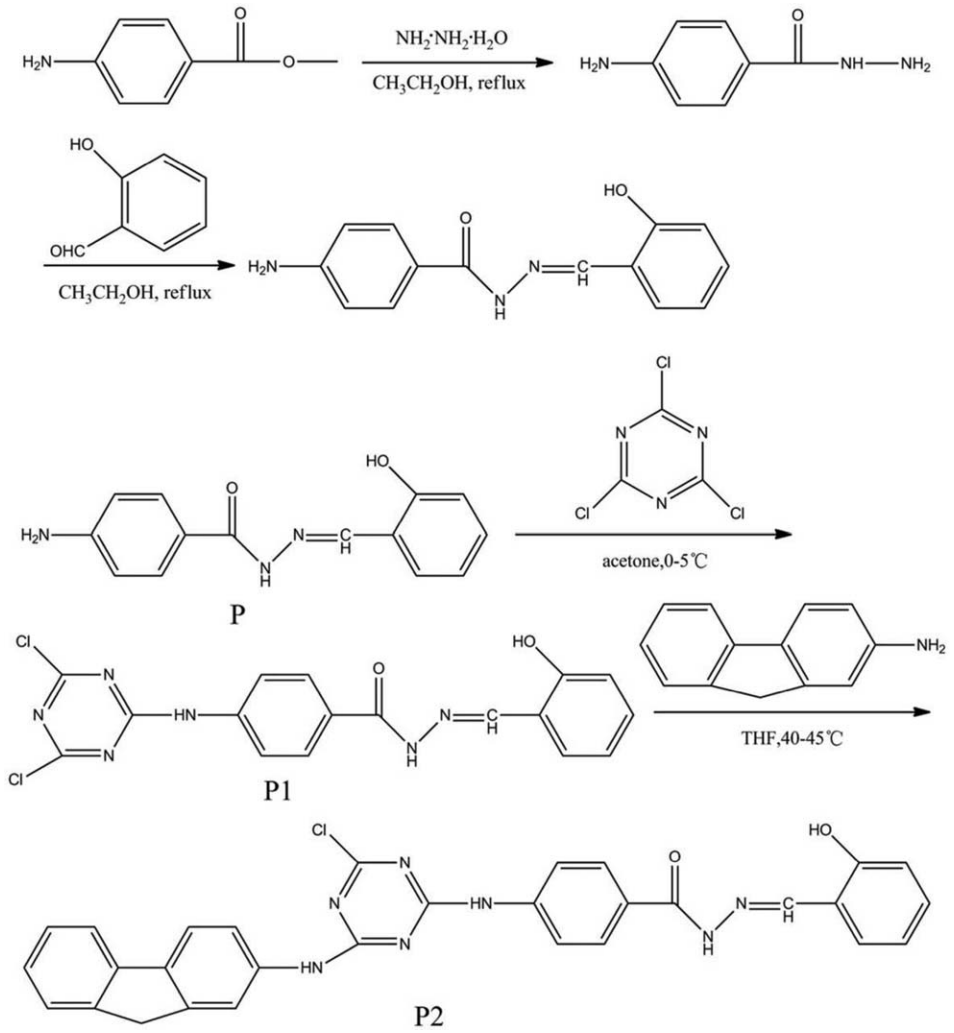

Figure 1. Synthesis routes of reactive dyes (P1, P2).

EXPERIMENTAL

Materials

Silk was supplied from silk factory of Qingyang City in China. 2,4,6-Trichloro-[1,3,5] triazine (98%) and 2-aminofluorene (99%) were purchased from J&K Scientific. Hydrazine hydrate (98%) was purchased from Alfa Aesar. Salicylaldehyde, *p*-amino benzoic acid methyl ester, ethanol, and sodium bicarbonate were analytical grade and purchased from Shanghai Pharmaceutical Corporation. All the reagents were used without further purification.

Synthesis of Reactive Dyes

The synthesis routs of reactive dyes were shown in Figure 1.

Synthesis of 4-amino hydrazone salicylaldehyde benzohydrazide (P): About 2.000 g (13.2 mmol) of methyl *p*-aminobenzoic acid was dissolved in 20.0 mL anhydrous ethanol, then 1.0 mL (19.8 mmol) 98% hydrazine hydrate was added dropwise. The mixture was refluxed for 4 h. The excessive hydrazine hydrate was removed using a rotary evaporator to give the crude product. The white crystals of aminobenzoyl hydrazide were obtained after recrystallization in ethanol. Then 1.600 g (10.5 mmol) aminobenzoyl hydrazide was dissolved in 20.0 mL ethanol. After that, 1.3 mL (11.0 mmol) 98% salicylaldehyde was added dropwise and the solution was refluxed for 0.5 h. The golden flaky crystals of P were obtained after recrystallization in ethanol to give a yield of 86.0%. mp: 139–140 °C. FTIR (KBr): $\nu = 3440$ cm^{-1} (OH); 1720 cm^{-1} (C═O); 1625 cm^{-1} (C═N); 1289 cm^{-1} (CN); 3041,1604,1571 cm^{-1} (Ar-H). ^{1}H NMR (400 MHz, DMSO, δ/ppm), 5.76 (2H, s), 6.96–7.03 (2H, m), 7.40–7.48 (1H, m), 7.54–7.52 (1H, d, $J = 8.2$ Hz), 7.70–7.72 (2H, d, $J = 7.9$ Hz), 8.04–8.06 (2H, d, $J = 8.6$ Hz), 9.01 (1H, s), 11.13 (1H, s), 12.65 (1H, s).

Synthesis of P1: 1.030 g (4.0 mmol) P was dissolved in 20.0 mL acetone in an ice-salt bath of 0–5 °C. Then 0.730 g (4.0 mmol) 2,4,6-Trichloro-[1,3,5] triazine was dissolved in 15.0 mL acetone and added dropwise to the above solution. The mixture was stirred at 0–5 °C for 2 h. 0.330 g (4.0 mmol) $NaHCO_3$ in aqueous solution was added to prevent the solution becoming acidic during the reaction. The product was filtered and repeatedly washed with small amount of acetone, then dried in a vacuum oven at 50 °C to afford a pale yellow powder of P1 at a yield of 72.3%. mp: 198–199 °C. FTIR (KBr): $\nu = 3448$ cm^{-1}

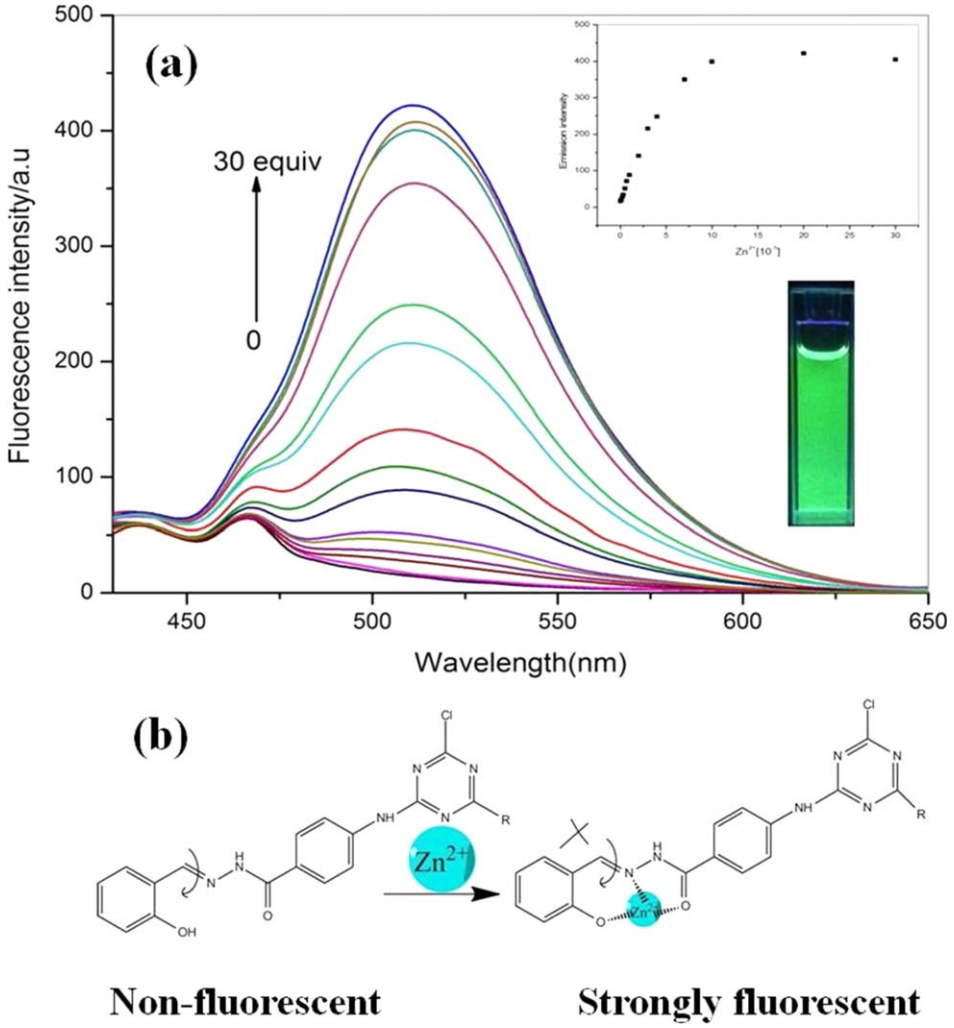

Figure 2. (a) Fluorescence spectra of P1 (10 μ*M*) upon addition of Zn^{2+} with an excitation of 415 nm. Inset shows the picture of P1-Zn^{2+} taken under 365 nm UV light in DMF solution. (b) Mechanism illustration of P1 for sensing Zn^{2+}. [Color figure can be viewed in the online issue, which is available at wileyonlinelibrary.com.]

(OH); 3283 cm^{-1} (NH); 1696 cm^{-1} (C═O); 3053, 1609, 1538 cm^{-1} (Ar-H); 1516, 1434 1387 cm^{-1} (triazine) ^{1}H NMR (400 MHz, DMSO, δ/ppm): 5.75 (2H, s), 7.76–7.80 (4H, m), 7.94–8.01 (4H, m), 10.94 (1H, s), 11.32 (1H, s).

Synthesis of P2: 0.200 g (1.09 mmol) 2-aminofluorene was dissolved in 5.0 mL tetrahydrofuran (THF) in an oil bath of 40–45 °C. 0.403 g (1.0 mmol) P1 in 15.0 mL THF was added dropwise to the above solution and stirred for 3 h. 0.085 g (1.0 mmol) $NaHCO_3$ in aqueous solution was added to prevent the solution becoming acidic during the reaction. The product was filtered and dissolved in 6. 0 mL THF, then added dropwise to 120.0 mL petroleum ether under stirring. The precipitate was filtered and dried in a vacuum oven at 50 °C to give a white solid powder of P2 at a yield of 69.0%. mp: 237–238 °C. FTIR (KBr): ν = 3420 cm^{-1} (OH); 3304 cm^{-1} (NH); 2955 cm^{-1} (CH_2); 1707 cm^{-1} (C═O); 3059,1611,1552 cm^{-1} (Ar—H); 1516,1441,1417 cm^{-1} (triazine). ^{1}H NMR (400 MHz, DMSO, δ/ppm): 3.84 (2H, s), 3.91 (2H, br), 7.31–7.27 (2H, t, J = 15.9 Hz), 7.40–7.36 (2H, t, J = 15.7 Hz), 7.58–7.57 (2H, d, J = 7.4 Hz), 7.98–7.77 (9H, m), 10.53 (1H, s), 10.89 (1H, s), 11.47 (1H, s).

Preparation of Functional SF Fabric

The nonwoven silk fabrics were prepared according to our previous study.[33] Then 1.0 g nonwoven silk fabrics were pre-wollen in 10 g/L NaOH solution. The nonwoven silk was first dyed in 0.04 g P1 or P2 solution at 30 °C for 1 h, then the temperature was increased to 60 °C (P1)/90 °C (P2) at a rate of 2 °C/min and incubated for 10 min. Finally, the silk fabrics were washed by water, dried, and used for their characterization:

$$E = (A_0 - A_1)/A_0 \times 100\% \quad (1)$$

$$R = (A_0 - A_1 - A_2)/(A_0 - A_1) \times 100\% \quad (2)$$

$$F = E \times R \quad (3)$$

The percentage of dyebath exhaustion (E) was calculated using eq. (1), where A_0 and A_1 were the absorbance of the dye solution before and after the dyeing process, respectively. The reaction percentage of the dyes (R) was calculated using eq. (2) and

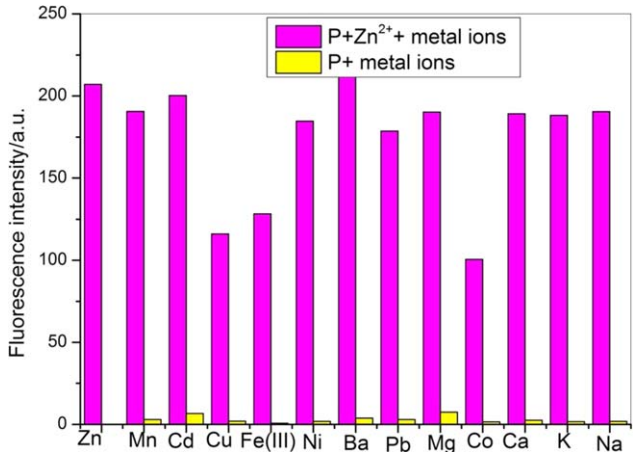

Figure 3. Fluorescence intensity of P1 (10 μ*M*) at 503 nm in the presence of various metal ions including zinc (10 μ*M*). Yellow bars represent the addition of various metal ions to P1. The magenta bars represent the addition of various metal ions to P1 and Zn^{2+} solution. The excitation wavelength was 415 nm. [Color figure can be viewed in the online issue, which is available at wileyonlinelibrary.com.]

the fixation of the reactive dyes (*F*) was calculated using eq. (3), where A_2 was the absorbance of the dyes in the rinsed water. The fixations of P1 and P2 were calculated as 42.2% and 39.6%, respectively.

Characterization

FTIR spectra were recorded in the region of 4000–400 cm^{-1} with the resolution of the scan as 4 cm^{-1} on a Nicolet NEXUS 8700 FTIR spectrophotometer using KBr disks at room temperature. ^1H NMR (400 MHz) spectra were measured on a Bruker DMX-400 NMR spectrometer using DMSO-d_6 as the solvent. UV-Vis absorption spectra were record on a Lambda 35 UV/Visspectrometer (Perkin Elmer) with a 1 cm quartz cell. The fluorescent spectra were measured by using LS 55 fluorescence spectrometer (Perkin Elmer) at a scanning rate of 500 nm/min.

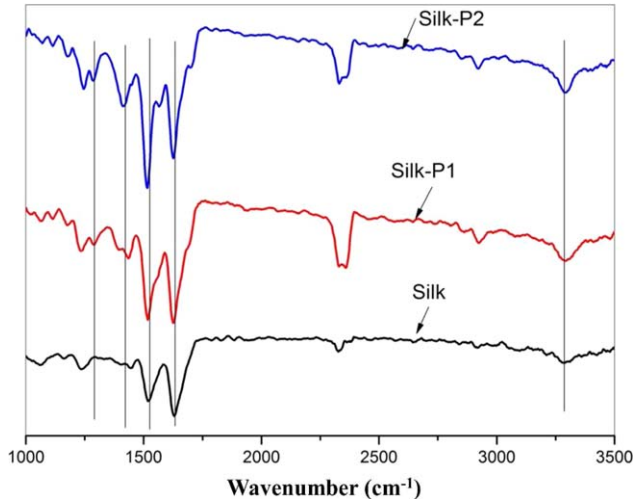

Figure 4. FTIR-ATR spectra of functional silk fabrics. [Color figure can be viewed in the online issue, which is available at wileyonlinelibrary.com.]

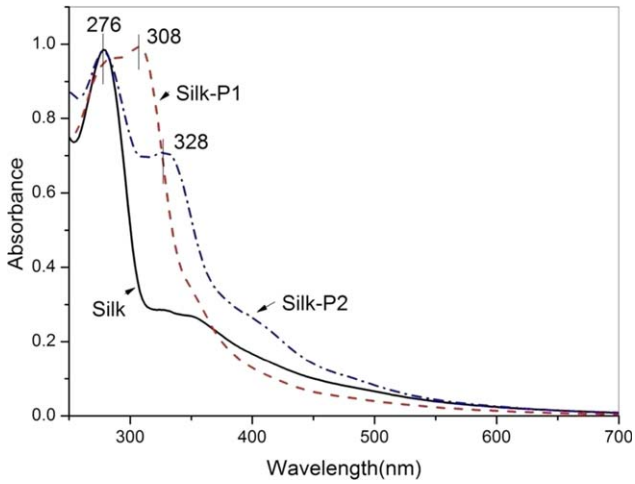

Figure 5. UV-Vis absorption spectra of functional silk fabrics. [Color figure can be viewed in the online issue, which is available at wileyonlinelibrary.com.]

RESULTS AND DISCUSSION

Synthesis and Characterization of Reactive Dyes

Two triazine-based reactive dyes (P1 and P2) were synthesized from 2,4,6-Trichloro-[1,3,5] triazine and 4-amino hydrazone salicylaldehyde benzohydrazide (P) through condensing reaction, which were characterized by FTIR and ^1H NMR. These data are listed in Experimental section, indicative of our successful synthesis. The remaining chlorines of P1 and P2 are used to functionalize the silk fabrics, while the unit of P gives them the capacity of sensing Zn^{2+}.

Taking P1 as an example, the sensing properties of P1 for Zn^{2+} detection were investigated. As shown in Figure 2(a), upon addition of Zn^{2+}, the fluorescent intensity at 503 nm became strong at a excitation wavelength of 415 nm, suggesting a large Stokes shifts of 88 nm, which is significant in the use of fluorescent probes. After the molar ratio of Zn^{2+} to P1 was about 20, the fluorescent intensity reached a maximum value, then almost kept constant or slightly decreased when further increasing Zn^{2+} concentration. According to Stern-Volmer equation, the linear correlation range and detection limit of Zn^{2+} were calculated (Supporting Information Figure S1). P1 had a linear range of 1 −10 μ*M* with a detection limit of 3 μ*M* (calculated by 3σ/slope), while P2 showed a linear range of 0.1–5 μ*M* with a detection limit of 1 μ*M*. Here we would like to compare our data with that in recent reports. Kim *et al.* synthesized an anthracene-based fluorescent chemosensor for Zn^{2+} with a detection limit of 2.4 μ*M*.[23] Zhang *et al.* synthesized a pyrazoline-based fluorescent probe for Zn^{2+} in aqueous solution with a detection limit of 0.8 μ*M*.[22] Xie *et al.* prepared a fluorescent probe for Zn^{2+} based on aggregation induced emission with a detection limit as low as 0.1 μ*M*.[21] More recently, Iniya *et al.* synthesized a triazole based fluorescent probe for Zn^{2+} and its detection limit was 0.42 μ*M*.[24] The above results demonstrated that P1 and P2 had high sensitivity of Zn^{2+}, which can be used as fluorescent probes for quantitative detection of Zn^{2+}.

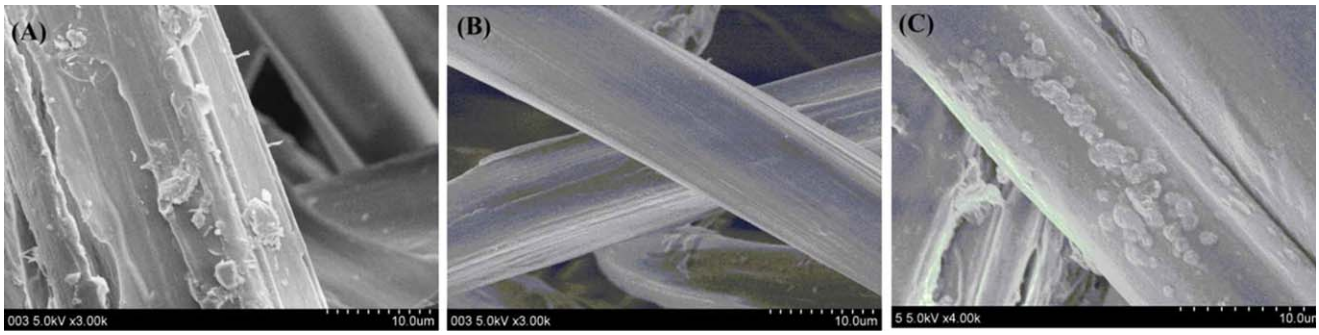

Figure 6. Scanning electron microscope images of silk fibers before and after soaking in DMF for 24h. (a) Silk fibers prepared by physical absorption of P1, (b) Silk fibers by P1 adsorption after soaking. (c) Silk-P1 after soaking in DMF. [Color figure can be viewed in the online issue, which is available at wileyonlinelibrary.com.]

The titration experiment (Job's Plot) was conducted to determine the binding ratio of P1 and Zn^{2+}. Keeping the total concentration of P1 and Zn^{2+} was 50 μ*M* here, the fluorescent intensity was measured by changing Zn^{2+} content. It was found that the fluorescent intensity was the strongest when the molar proportion of Zn^{2+} was at 0.5 (Supporting Information Figure S2). Thus the binding ratio of P1 and Zn^{2+} was 1:1. The probe mechanism of P1 for sensing Zn^{2+} was illustrated in Figure 2(b). In the absence of Zn^{2+}, P1 is nonfluorescent because C═N isomerization is the predominant decay process of in excited states. After the formation of the complex between P1 and Zn^{2+}, the rotation of C═N bond was restricted and C═N isomerization was surpressed,[8,9,34] resulting in enhanced planarity and rigidity, thus the strong fluorescence was observed.

High selectivity is another important parameter for an excellent fluorescent probe. The ion selectivity of P1 was shown in Figure 3. In the presence of other metal ions except Zn^{2+}, including Mn^{2+}, Cd^{2+}, Cu^{2+}, Fe^{3+}, Ni^{2+}, Ba^{2+}, Pb^{2+}, Mg^{2+}, Co^{2+}, Ca^{2+}, K^{+}, and Na^{+}, fluorescence turn-on was not observed even at high ion concentrations or with the combination of them, indicating that P1 had a high selectivity on Zn^{2+} detection. Moreover, when other metal ions were added to P1 in the presence of Zn^{2+}, most of the metal ions didn't show any interference except Cu^{2+}, Fe^{3+}, and Co^{2+}, probably because of their competition with Zn^{2+} to form the complex with P1. Thus the above results suggested that the reactive dyes had high sensitivity and selectivity in the detection of Zn^{2+}.

Preparation and Characterization of Functional Silk Fabric

Functional silk fabrics were prepared by using the above reactive dyes via the dyeing process, as described in Experimental section. Figure 4 presents FTIR spectra of functional silk fibers (silk-P1 and silk-P2). Besides the absorption bands at 3350, 1630–1650, and 1540–1520 cm^{-1} from raw silk fabrics, which originated from the intra/inter molecular hydrogen bonding interactions of —OH and —NH_2 groups, Amide I and Amide II, respectively, new absorption bands at 1346 and 1473 cm^{-1} in silk-P1 and that at 1336 and 1467 cm^{-1} in silk-P2 were attributed to triazine groups, suggesting that P1 and P2 have been successfully introduced into silk fabrics.

Figure 5 shows the ultraviolet-visible absorption spectrum of functional silk fabrics. Besides the absorption peak at 276 nm from raw silk fabrics, absorption peaks located at 308 and 328 nm came from P1 and P2, respectively, also indicating that P1 and P2 have been introduced into silk fabrics. The 20 nm red shift of P2 compared with P1 was attributed to the hyperconjugation of fluorene unit. In order to verify whether reactive dyes were covalent connection to silk fabrics, functional silk fabrics were soaking in DMF for 24 h. Figure 6 shows scanning electron microscope images of silk fibers before and after soaking. When P1 was introduced into silk fabrics by physical absorption [Figure 6(a)], reactive dyes were almost completely desorbed after soaking, and the surface of silk fibers became smooth [Figure 6(b)]. However, P1 still existed on the surface of Silk-P1 after soaking, indicating that P1 was connected to

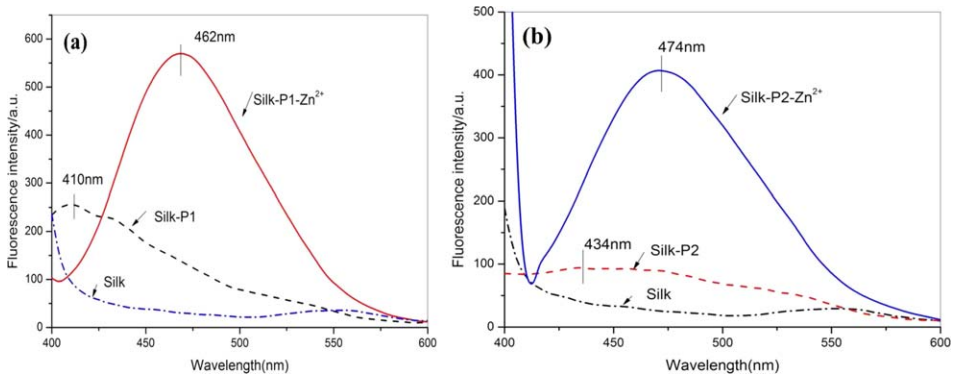

Figure 7. Fluorescence spectra of (a) silk-P1 and (b) silk-P2 upon addition of Zn^{2+} with an excitation wavelength of 405 nm. [Color figure can be viewed in the online issue, which is available at wileyonlinelibrary.com.]

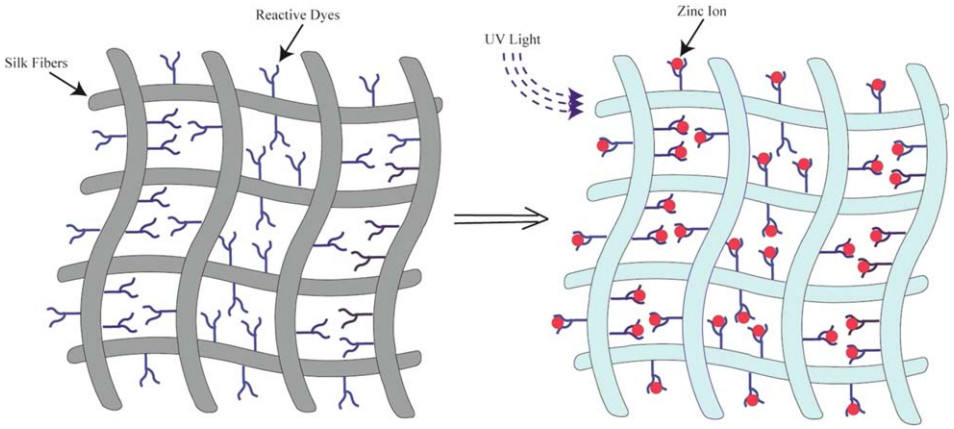

Figure 8. Schematic illustration of functional nonwoven silk fabrics for Zn^{2+} detection and absorption. [Color figure can be viewed in the online issue, which is available at wileyonlinelibrary.com.]

silk fibers through chemical bonding in Silk-P1, rather than physical adsorption. UV spectra (Supporting Information Figure S3) further confirmed this conclusion. The prepared functional silk fabrics here showed negligible change after soaking, while silk fabrics by physical absorption of P1 and P2 exhibited an obvious desorption of reactive dyes.

Application of Functioal Silk Fabric in Zn(II) Detection and Absorption

Reactive dyes P1 and P2 were good sensors of Zn(II), thus the application of silk-P1 and silk-P2 in Zn(II) detection were investigated. Figure 7 shows fluorescence spectra of silk-P1 and silk-P2 upon addition of Zn^{2+}. Compared with the raw silk fibers, a weak fluorescence at 410 nm ($\lambda_{ex} = 365$ nm) was observed in silk-P1, which originated from P1. After addition of zinc ions, a strong fluorescence ($\lambda_{ex} = 405$ nm) at 462 nm occurred. As a result, the fabrics exhibited cyanine under UV irritation (Supporting Information Figure S4). Analogously, silk-P2 showed a weak fluorescence emission peak at 434 nm, while strong fluorescence emission peak ($\lambda_{ex} = 405$ nm) at 474 nm was observed after complexation with zinc ion. The above results demonstrated that these functional silk fabrics can be used to detect Zn^{2+}.

Besides fluorescent detection of Zn^{2+}, the absorption capacity of nonwoven silk fabric was also evaluated, as illustrated in Figure 8. At room temperature (27 °C), 1 g modified and unmodified nonwoven silk fabrics were immersed in an aqueous solution of zinc ions (100 mL, 20 mmol/L) for 30 h. The zinc ion concentration was measured using inductively coupled plasma atomic emission analyzer. The adsorption capacity of zinc ions was calculated according to the following equation: $Q = (C_b - C_a)V/Mm$, where Q is the adsorption capacity of silk fabric (mmol zinc ions/g silk); C_b and C_a were zinc ion concentration before and after adsorption test (mg/L), respectively; V is the volume (L) of Zn^{2+} solution; M is the molecular weight of the Zn^{2+} (g/mol); m is the weight of the silk fibers (g). The results showed that the Zn^{2+} absorption capacity of silk-P1 and silk-P2 was 0.50 mmol/g, 0.49 mmol/g, about 1.3 times as the raw silk fabric (0.38 mmol/g), suggesting that the adsorption capacity of zinc ion was significantly improved after chemical modification by using reactive dyes. In the silk-P1, the content of reactive dyes is 0.042 mmol/g after considering its fixation. While the Zn^{2+} absorption capacity was increased by 0.12 mmol/g for silk-P1, much larger than that of Zn^{2+} absorption by the binding of dyes considering that their binding ratio is 1. The above results suggest that chemical modification of silk fabric by reactive dyes not only increase Zn^{2+} absorption by the binding of dyes, but also enhance the Zn^{2+} absorption capacity of silk fabric itself, which may be because of the decreased degree of crystallinity.

CONCLUSIONS

Here functional silk fabrics were prepared via chemical modification by using two reactive dyes, which were good fluorescent probes of Zn^{2+}. Consequently, nonwoven fabric of functional silk fibers exhibited good applications in fluorescent detection and absorption of Zn^{2+}. Because of the good biocompatibility of SF, the prepared functional silk fabrics here are expected to be used in biological applications, e.g. fluorescent sensor of Zn^{2+} *in vivo*.

ACKNOWLEDGMENTS

This research was financially supported by the National Natural Science Fund of China (Grant Nos. 21471030, 21271040 and 21171034), Shanghai Municipal Natural Science Foundation for Youths (No. 12ZR144100) and "Chen Guang" project (No. 12CG37) supported by Shanghai Municipal Education Commission and Shanghai Education Development Foundation.

REFERENCES

1. Lim, N. C.; Freake, H. C.; Bruckner, C. *Chem. Eur. J.* **2005**, *11*, 38.
2. Frederickson, C. J.; Hernandez, M. D.; Mcginty, J. F. *Brain Res.* **1989**, *480*, 317.
3. Bush, A. I.; Pettingell, W. H.; Multhaup, G.; Paradis, M. D.; Vonsattel, J. P.; Gusella, J. F.; Beyreuther, K.; Masters, C. L.; Tanzi, R. E. *Science* **1994**, *265*, 1464.

4. Gao, C. J.; Jin, X. J.; Yan, X. H.; An, P.; Zhang, Y.; Liu, L. L.; Tian, H.; Liu, W. S.; Yao, X. J.; Tang, Y. *Sens. Actuators B Chem.* **2013**, *176*, 775.
5. Zhang, Y.; Guo, X. F.; Si, W. X.; Jia, L. H.; Qian, X. H. *Org. Lett.* **2008**, *10*, 473.
6. Du, J. J.; Fan, J. L.; Peng, X. J.; Li, H. L.; Sun, S. G. *Sens. Actuators B Chem.* **2010**, *144*, 337.
7. Sutariya, P. G.; Modi, N. R.; Pandya, A.; Joshi, B. K.; Joshi, K. V.; Menon, S. K. *Analyst* **2012**, *137*, 5491.
8. Song, Z. K.; Dong, B.; Lei, G. J.; Peng, M. J.; Guo, Y. *Tetrahedron Lett.* **2013**, *54*, 4945.
9. Wu, J. S.; Liu, W. M.; Zhuang, X. Q.; Wang, F.; Wang, P. F.; Tao, S. L.; Zhang, X. H.; Wu, S. K.; Lee, S. T. *Org. Lett.* **2007**, *9*, 33.
10. Xu, Z. C.; Liu, X.; Pan, J.; Spring, D. R. *Chem. Commun.* **2012**, *48*, 4764.
11. Li, H. Y.; Gao, S.; Xi, Z. *Inorg. Chem. Commun.* **2009**, *12*, 300.
12. Liu, Z. H.; Tonnele, C.; Battagliarin, G.; Li, C.; Gropeanu, R. A.; Weil, T.; Surin, M.; Beljonne, D.; Lazzaroni, R.; Debliquy, M.; Renoirt, J. M.; Mullen, K. *J. Phys. Chem. B* **2014**, *118*, 309.
13. Taki, M.; Watanabe, Y.; Yamamoto, Y. *Tetrahedron Lett.* **2009**, *50*, 1345.
14. Kursunlu, A. N.; Guler, E.; Ucan, H. I.; Boyle, R. W. *Dyes Pigments* **2012**, *94*, 496.
15. Zhu, S. L.; Zhang, J. T.; Janjanam, J.; Vegesna, G.; Luo, F. T.; Tiwari, A.; Liu, H. Y. *J. Mater. Chem. B* **2013**, *1*, 1722.
16. Cao, J.; Zhao, C. C.; Wang, X. Z.; Zhang, Y. F.; Zhu, W. H. *Chem. Commun.* **2012**, *48*, 9897.
17. Zhang, J. F.; Bhuniya, S.; Lee, Y. H.; Bae, C.; Lee, J. H.; Kim, J. S. *Tetrahedron Lett.* **2010**, *51*, 3719.
18. Kong, L.; Chen, Y.; Ye, W. B.; Zhao, L.; Song, B.; Yang, J. X.; Tian, Y. P.; Tao, X. T. *Sens. Actuators B Chem.* **2013**, *177*, 218.
19. Yin, S. C.; Zhang, J.; Feng, H. K.; Zhao, Z. J.; Xu, L. W.; Qiu, H. Y.; Tang, B. Z. *Dyes Pigments* **2012**, *95*, 174.
20. Wang, L. N.; Qin, W. W.; Tang, X. L.; Dou, W.; Liu, W. S. *J. Phys. Chem. A* **2011**, *115*, 1609.
21. Xie, D. X.; Ran, Z. J.; Jin, Z.; Zhang, X. B.; An, D. L. *Dyes Pigments* **2013**, *96*, 495.
22. Zhang, T. T.; Wang, F. W.; Li, M. M.; Liu, J. T.; Miao, J. Y.; Zhao, B. X. *Sens. Actuators B Chem.* **2013**, *186*, 755.
23. Kim, J. H.; Noh, J. Y.; Hwang, I. H.; Kang, J.; Kim, J.; Kim, C. *Tetrahedron Lett.* **2013**, *54*, 2415.
24. Iniya, M.; Jeyanthi, D.; Krishnaveni, K.; Mahesh, A.; Chellappa, D. *Spectrochim. Acta A* **2014**, *120*, 40.
25. Gil, E. S.; Panilaitis, B.; Bellas, E.; Kaplan, D. L. *Adv. Healthc. Mater.* **2013**, *2*, 206.
26. Zhong, T. Y.; Xie, Z. G.; Deng, C. M.; Chen, M.; Gao, Y. F.; Zuo, B. Q. *J. Appl. Polym. Sci.* **2013**, *127*, 2019.
27. Chutipakdeevong, J.; Ruktanonchai, U. R.; Supaphol, P. *J. Appl. Polym. Sci.* **2013**, *130*, 3634.
28. Asakura, T.; Saotome, T.; Aytemiz, D.; Shimokawatoko, H.; Yagi, T.; Fukayama, T.; Ozai, Y.; Tanaka, R. *RSC Adv.* **2014**, *4*, 4427.
29. Tang, B.; Li, J. L.; Hou, X. L.; Afrin, T.; Sun, L.; Wang, X. G. *Ind. Eng. Chem. Res.* **2013**, *52*, 4556.
30. Lin, N. B.; Liu, X. Y.; Diao, Y. Y.; Xu, H. Y.; Chen, C. Y.; Ouyang, X. H.; Yang, H. Z.; Ji, W. *Adv. Funct. Mater.* **2012**, *22*, 361.
31. Lin, N. B.; Hu, F.; Sun, Y. L.; Wu, C. X.; Xu, H. Y.; Liu, X. Y. *Adv. Funct. Mater.* **2014**, *24*, 5284.
32. Lin, N. B.; Meng, Z. H.; Toh, G. W.; Zhen, Y.; Diao, Y. Y.; Xu, H. Y.; Liu, X. Y. *Small* **2015**, *11*, 1205.
33. Guang, S. Y.; An, Y.; Ke, F. Y.; Zhao, D. M.; Shen, Y. H.; Xu, H. Y. *J. Appl. Polym. Sci.* **2015**, *132*, 42503.
34. Wu, J.; Liu, W.; Ge, J.; Zhang, H.; Wang, P. *Chem. Soc. Rev.* **2011**, *40*, 3483.